Electrochemistry Communications 98 (2019) 6–9

Contents lists available at ScienceDirect

Electrochemistry Communications

journal homepage: www.elsevier.com/locate/elecom

Production and printing of graphene oxide foam ink for electrocatalytic applications

Luis Baptista-Pires[a], Alfredo de la Escosura-Muñiz[a], Marc Balsells[a], Julio C. Zuaznabar-Gardona[b], Arben Merkoçi[a,c,*]

[a] Catalan Institute of Nanoscience and Nanotechnology (ICN2), CSIC and BIST, Campus UAB, Bellaterra, 08193 Barcelona, Spain
[b] Nanobiotechnology & Bioanalysis Group, Departament d' Enginyeria Química, Universitat Rovira i Virgili, Avinguda Països Catalans 26, 43007 Tarragona, Spain
[c] ICREA, Pg. Lluís Companys 23, 08010 Barcelona, Spain

ARTICLE INFO

Keywords:
Graphene
Ink
Foam
Print
Electrocatalysis
Sensors

ABSTRACT

A graphene-based ink printed as a foam-like structure with open pores is reported. The production of the ink is easier and faster than using existing methods and the obtained product is stable in water suspension. Electrocatalytic applications of 3D structured electrodes printed onto plastic substrates were explored.

1. Introduction

Graphene-based materials exist in a variety of forms that include 0D, 1D, planar 2D and 3D structures [1]. 3D graphene structures such as graphene-based foams have been much studied in recent years due to the remarkable electrical and mechanical properties associated with their 3D structure, which has a large surface area. Graphene oxide (GO) is a material known for its high yield production process, defective structure and insulating electronic properties due to the presence of large numbers of oxygen functional groups. These groups can be removed using reducing agents and the resulting material, reduced graphene oxide (RGO), is conductive with semi-metallic-like behavior. RGO-based foams can be produced using innovative reducing strategies. Z. Niu et al. have obtained RGO foams by simple vacuum filtration followed by reduction of GO in hydrazine solution by autoclaving at 90 °C for 10 h, resulting in a horizontal porous network from sub micrometer to micrometer scales that is cross linked without a complete separation between the different layers. This foam has a low electrical resistance of less than 100 Ω/square [2]. In a different approach, Pirkle et al. mixed 1 M KOH into a GO suspension and heated at 100 °C under constant stirring until a paste was obtained. This paste can be simply filtered in vacuum and reduced further. The resulting porous film is flexible, highly conductive and can be cut into desired shapes. The KOH concentration seems to be a key factor in obtaining homogeneous films [3,4]. Another way of producing RGO foams is through hydrothermal reduction. Briefly, 50 mL of 2 g/L GO aqueous dispersion is sealed in a Teflon-lined autoclave and maintained at 150 °C for 5 h; the autoclave is then cooled to room temperature, resulting in a three-dimensional (3D) RGO hydrogel [5]. In a different approach aimed at producing 3D cellular films for supercapacitor applications, the methodology consists of pre-reduction of GO sheets, then filtering using vacuum filtration, followed by dropping the film into liquid nitrogen to solidify, causing the GO sheets to form a 3D structure [6]. Another approach using vacuum filtration for the production of thin films through direct laser writing has been reported [7,8]. GO-based foam composites have also been tested for use as a fire retardant [9]. Herein we propose a novel methodology using a short (45 min) autoclave-based procedure for the production of RGO foams; these are then suspended in water and sonicated. The resulting foam-like matrix can be printed over plastics using wax-printed membrane based technology. This material should be of great interest for electronic applications in energy and (bio)sensor research due to its large surface area, electrochemical behavior, flexibility and transparency.

2. Experimental

The nitrocellulose membranes used are hydrophilic, with a pore size of 0.025 µm and a diameter of 47 mm. The wax was printed with a Xerox ColorQube 8570 printer using the high resolution printing mode. The electrode patterns were created using Corel Draw.

* Corresponding author at: Catalan Institute of Nanoscience and Nanotechnology (ICN2), CSIC and BIST, Campus UAB, Bellaterra, 08193 Barcelona, Spain.
E-mail address: arben.merkoci@icn2.cat (A. Merkoçi).

https://doi.org/10.1016/j.elecom.2018.11.001
Received 28 September 2018; Received in revised form 1 November 2018; Accepted 1 November 2018
Available online 10 November 2018
1388-2481/ © 2018 Elsevier B.V. This is an open access article under the CC BY-NC-ND license (http://creativecommons.org/licenses/BY-NC-ND/4.0/).

Commercially available GO solution with a concentration of 5 mg/mL was obtained from Angstrom Materials (N002-PS-0.5) and diluted in water to a concentration of 1 mg/mL. To prepare the RGO foam and transfer it onto a plastic substrate, 100 mL of a 1 mg/mL GO solution was mixed with 100 mL of 1 mg/mL of ascorbic acid (Sigma-Aldrich), followed by autoclaving at 125 °C for 45 min. Material was obtained from the remaining RGO agglomerated in water solution after autoclave treatment and transferred to a 50 mL plastic flask filled with 40 mL of water and sonicated for 15 min at 20 Hz using a probe sonicator (Qsonica Q125). The resulting solution was left at room temperature for 1 day in order to precipitate the unsuspended particles. The aqueous suspension of RGO was then filtered through wax-printed membranes using a 1 L vacuum-filtering flask, 300 mL glass filter holder and 47 mm SS screen (1/Pk). The RGO-modified wax-printed membranes (WPMs) were transferred using the roller-to-roller system used for paper transport in the wax-based printer.

The samples were electrochemically characterized with $K_3[Fe(CN)_6]$ (Sigma-Aldrich) as redox probe in KNO_3 (Sigma-Aldrich) as supporting electrolyte using an Autolab302 potentiostat/galvanostat/frequency-response analyzer PGST30, controlled by GPES/FRA Version 4.9. The X-ray photoelectron spectroscopy (XPS) measurements were performed with a Phoibos 150 analyzer (SPECS GmbH, Berlin, Germany) under ultrahigh vacuum conditions (base pressure 1×10^{-10} mbar) with a monochromatic aluminum Kα X-ray source (1486.74 eV). The energy resolution (as measured by the fwhm of the Ag 3d5/2 peak for a sputtered silver foil) was 0.58 eV. Scanning electron microscopy (SEM) was carried out on a FEI Quanta FEG (pressure, 70 Pa; HV, 20 kV; and spot, four).

16 nm gold nanoparticles (AuNPs) were synthesized by reducing tetrachloroauric acid (Sigma-Aldrich) with trisodium citrate (Sigma-Aldrich), a method pioneered by Turkevich [10]. Electrochemical detection of AuNPs was performed by placing 50 µL of the suspension of AuNPs in 1 M HCl (Sigma-Aldrich) and applying a potential of +1.35 V for 1 min (electrochemical pretreatment) followed by a potential of −1.00 V for 120 s in chronoamperometric mode [11].

3. Results and discussion

The experimental procedure for preparing the RGO foam and transferring it onto a plastic substrate is illustrated in Fig. 1. This involves mixing 100 mL of a 1 mg/mL GO solution with 100 mL of 1 mg/mL of ascorbic acid, followed by autoclaving. The autoclaving temperature and time were optimized by evaluation of the C/O ratio of the obtained material by C1s X-ray photoelectron spectroscopy (XPS). The data in Table 1 show that the C/O ratio increases with both time (at a fixed temperature of 125 °C) and temperature (at a fixed time of 45 min), reaching a plateau at a value of approximately 6.78 which is obtained by heating at 125 °C for 45 min. These were the conditions used for RGO reduction. The resulting material was characterized by SEM and is composed of a network of RGO sheets that upon drying at room temperature form a crumpled RGO (see Fig. 2a). However, once freeze dried (which can indicate the form after thermal treatment) it forms a cavity-like structure with stacked RGO layers (see Fig. 2b). The remaining RGO agglomerated in ascorbic acid solution after autoclave treatment was transferred to a 50 mL plastic flask filled with 40 mL of water and sonicated for 15 min at 20 Hz using a probe sonicator. The resulting solution was left at room temperature for 1 day in order to precipitate the unsuspended particles. The homogeneous water–RGO suspension was transferred to a different flask and remained stable for over a month.

Table 1
C/O ratio calculated from C1s XPS measurements for RGO-based foams obtained after autoclaving. The top part of the table gives results obtained with a constant temperature of 125 °C for different autoclaving times. The bottom part of the table gives results obtained with a constant time of 45 min for different autoclaving temperatures.

Time (min)	C/O ratio
1	3.69 ± 0.36
3	3.83 ± 0.22
5	3.95 ± 0.44
10	4.59 ± 0.42
15	5.52 ± 0.32
25	6.32 ± 0.11
35	6.56 ± 0.21
45	6.78 ± 0.17
60	6.82 ± 0.12

Temperature (°C)	C/O ratio
75	2.73 ± 0.29
100	3.20 ± 0.31
125	6.78 ± 0.17
150	6.80 ± 0.13

It is important to note that in the presented methodology we avoid

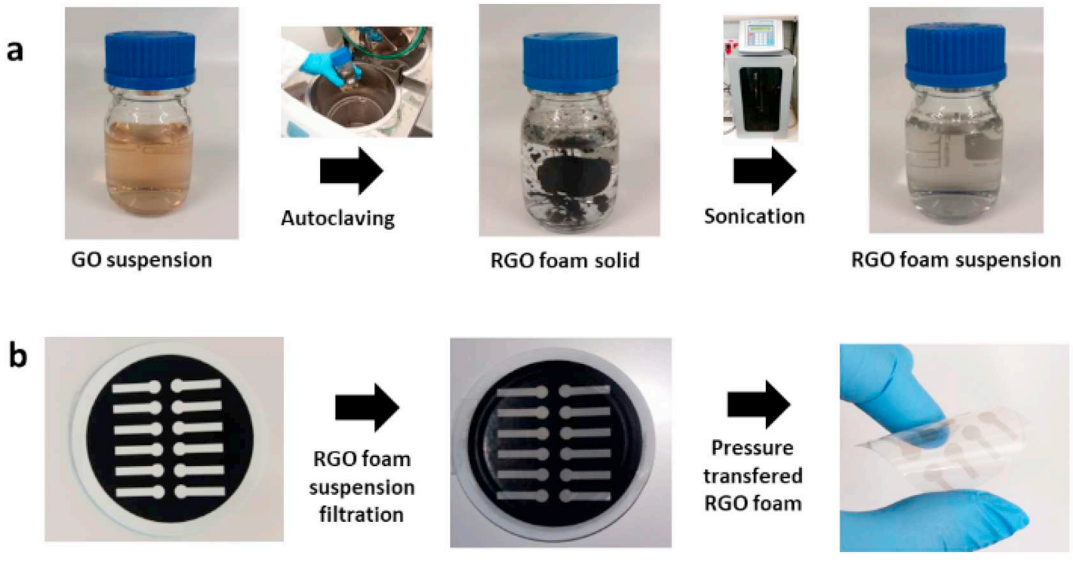

Fig. 1. Scheme showing (a) the experimental procedure for preparation of the RGO foam suspension and (b) its transfer onto a plastic substrate.

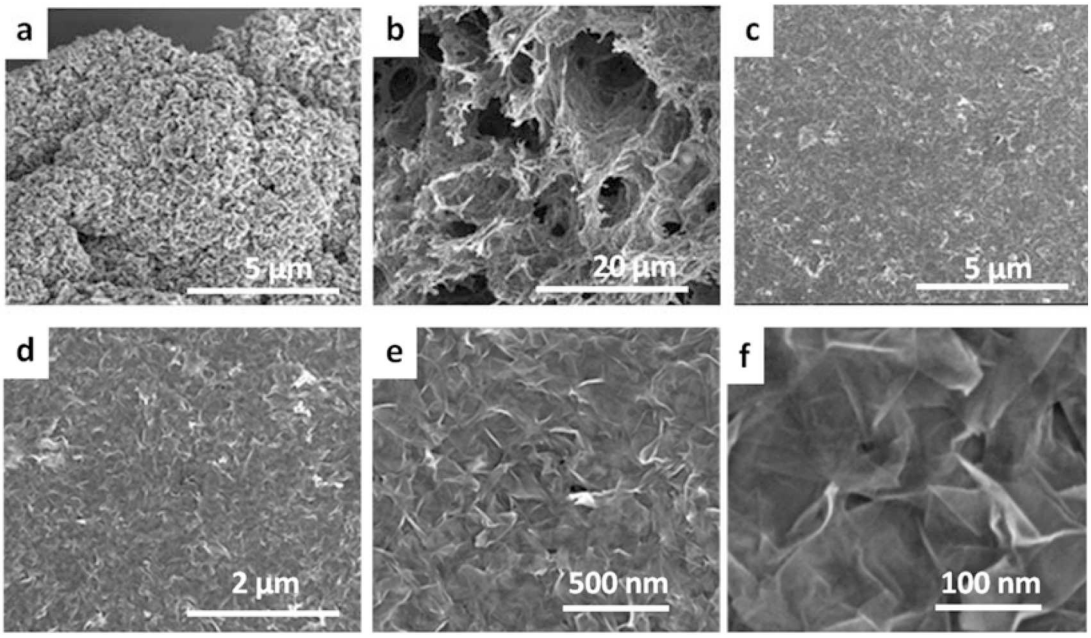

Fig. 2. SEM images of (a) the crumpled RGO formed upon drying at room temperature; and (b) the porous strucuture obtained after freeze drying. (c–f) SEM images (at different magnifications) of the open porous network obtained upon printing with the foam-based ink.

the drying step after the autoclave treatment and maintain the bulk foam form in water solution during the whole ink formulation process. The separation of the sheets upon sonication offers an innovative advantage, providing small clusters of RGO sheets approximately 200 nm in size suspended in water.

Printing using these foam-based inks was performed by adapting our previously reported technology using wax-printed membranes (Fig. 1b) [12]. Briefly, 5 mL of the ink were filtered and patterned using wax-printed membranes of the desired shape. The printing methodology consists of the filtration of a water suspension through the unclogged areas not covered by the wax. These areas enable the water to be filtered out, leaving a RGO film on the top of the membrane. These WPMs coated with RGO particles are placed over the target substrate and the back of the WPM is dried rapidly (for 10 s) using compressed air. To transfer the filtered RGO material, pressure is applied using the roller-to-roller mechanism in the wax printer, leaving the patterned structures on top of the substrates. The mechanism of passing the sample through the printer rollers from the manual feed tray could be substituted by a normal desktop laminator, as once demonstrated elsewhere by our group; no temperature is needed, only sufficient pressure to make contact between the filtered layer and the target substrate – even simply using pressure from a spatula or a finger [12,13]. Unlike other reported strategies, the ink made by the process reported here is stable in water for at least 1 month without the need for surfactants or additional solvents; the shaping capability introduces a step forward for printing sensors where the geometric area is important; and the roller-to-roller transfer process introduces the possibility of mass production and industrialization of one-step printing of porous 3D conductive films [13,14].

When the resulting foam-based ink is used for printing, an open porous network with a highly active surface area (Fig. 2c–f) is obtained. This may be due to the combination of the stable microclusters of RGO particles and the use of vacuum filtration technology.

The vacuum filtration process is faster for RGO than for GO as it does not clog the pores and there are open channels for the water to be filtered, resulting in shorter filtration times (compared with GO). This suggests that filtration is a building block in this open network. In addition, the 300 nm thick film does not have any room for shrinkage once it is attached to the substrate; this means the film is both compact (with highly interconnected RGO flakes) and porous (due to the filtration channels).

This material was also characterized electrochemically. Electrodes prepared using the method described above were evaluated by cyclic voltammetry in 2 mM $K_3[Fe(CN)_6]$/0.2 M KNO_3 using a three-electrode system, with Ag/AgCl as the reference electrode and a platinum wire counter electrode. As shown in Fig. 3a, a number of different scan rates in the range 2–100 mV/s were evaluated, revealing well-resolved anodic and cathodic peaks corresponding to the reversible $[Fe(CN)_6]^{4-}$ / $[Fe(CN)_6]^{3-}$ oxidation/reduction system. As shown in Fig. 3b, a straight line was observed on plotting the current intensity of both anodic and cathodic peaks against the square root of the scan rate, which is consistent with a diffusion-controlled redox process.

These data make it possible to estimate (using the well-known Randles-Sevcik equation) that the electrochemically active area is around 0.047 cm^2. This effective area is considerably higher than that calculated for standard screen-printed carbon electrodes (SPCEs) of the same geometric size (around 0.016 cm^2), probably due to the high porosity and 3D structure of the foam electrodes. Additionally, the standard heterogeneous rate constant of electron transfer (k^0) was estimated following the Nicholson method [15]. An average rate constant of $2.4*10^{-4}$ cm/s for the $[Fe(CN)_6]^{3-/4-}$ redox pair was obtained. Such values of k^0 were of the same order of magnitude as for tested commercially available SPCEs ($k^0 \sim 5*10^{-4}$ cm/s). These results illustrate the possibility of using the RGO foam as an excellent substrate for monitoring electrochemical processes.

The advantages of such electrodes were also evaluated by studying the hydrogen evolution reaction (HER) catalyzed by gold nanoparticles (AuNPs). This method was developed and used extensively in our group for the sensitive detection of AuNP tags in biosensing systems, using SPCE electrodes [11]. Chronoamperograms recorded at –1 V in 1 M HCl showed increased catalytic currents for different AuNPs concentrations in the range 59–3000 pM, as shown in Fig. 3c. A logarithmic relationship between the current intensity and the AuNP concentration was found in this range (Fig. 3d), allowing a detection limit of around 0.5 pM to be estimated. This is lower than that obtained experimentally with SPCEs (around 1 pM). The sensitivity of the detection system was also substantially better than the corresponding values for SPCEs as the slope of the curve is more than twice as large (Fig. 3d). These results are

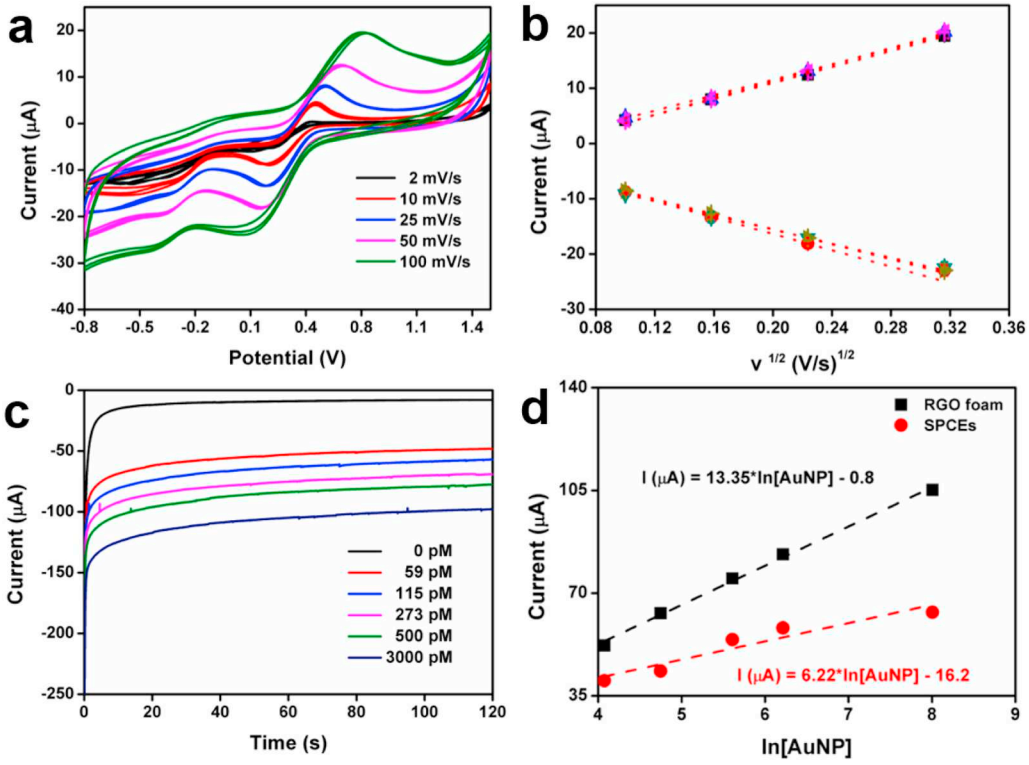

Fig. 3. Electrochemical characterization of the prepared RGO foam electrodes. (a) Cyclic voltammograms recorded in 2 mM $K_3[Fe(CN)_6]$ / 0.2 M KNO_3 at different scan rates in the range 2–100 mV/s. (b) Plot of current intensity of anodic and cathodic peaks vs the square root of the scan rate. (c) Chronoamperograms recorded at −1 V in 1 M HCl for different concentrations of AuNPs. (d) Relationship between the catalytic current intensity (recorded at 100 s) and the AuNP concentrations assayed for RGO foam electrodes and SPCEs.

in agreement with the high surface area observed for the foam electrodes. Another factor that could contribute to this excellent performance for electrocatalytic determination of AuNPs may be the high porosity of these electrodes, which could facilitate the release of hydrogen during the hydrogen evolution reaction, favoring the kinetics of this reaction and the mass transfer.

4. Conclusions

In summary, the ease of ink preparation, the resulting suspended microparticles or RGO clusters, and the stability of these in water constitute a step forward in ink formulation. The ability to print with this ink using wax-printed membranes makes it possible to produce RGO foam-like thin films of specific shape and thickness. The small, porous and connected RGO layers enable the electrical properties to be maintained while increasing surface area and edge-like exposure. The electrochemical properties were explored, revealing the ability to detect half the quantity of nanoparticles that a SPCE can detect for similar surface areas, demonstrating a significant improvement in sensitivity. The printed electrodes described here can be studied for use in a wide range of applications including sensors and energy, among others.

Acknowledgements

We acknowledge support from MINECO, Spain, for MAT2017-87202-P, the Severo Ochoa program (Grant No. SEV-2013-0295) and Graphene Flagship Core Project 2 (Ref: 785219). This work is also funded by the CERCA Programme/Generalitat de Catalunya.

References

[1] E. Morales-Narváez, L.F. Sgobbi, S.A.S. Machado, A. Merkoçi, Graphene-encapsulated materials: synthesis, applications and trends, Prog. Mater. Sci. 86 (2017) 1–24.
[2] Z. Niu, J. Chen, H.H. Hng, J. Ma, X. Chen, A leavening strategy to prepare reduced graphene oxide foams, Adv. Mater. 24 (30) (2012) 4144–4150.
[3] L.L. Zhang, X. Zhao, M.D. Stoller, Y. Zhu, H. Ji, S. Murali, Y. Wu, S. Perales, Br. Clevenger, R.S. Ruoff, Highly conductive and porous activated reduced graphene oxide films for high-power supercapacitors, Nano Lett. 12 (4) (2012) 1806–1812.
[4] Y. Zhu, S. Murali, M.D. Stoller, K.J. Ganesh, W. Cai, P.J. Ferreira, A. Pirkle, R.M. Wallace, K.A. Cychosz, M. Thommes, D. Su, E.A. Stach, R.S. Ruoff, Carbon-based supercapacitors produced by activation of graphene, Science 332 (6037) (2011) 1537–1541.
[5] J.L. Shi, W.C. Du, Y.X. Yin, Y.G. Guo, L.J. Wan, Hydrothermal reduction of three-dimensional graphene oxide for binder-free flexible supercapacitors, J. Mater. Chem. A 2 (2014) 10830–10834.
[6] Y. Shao, M.F. El-Kady, C.W. Lin, G. Zhu, K.L. Marsh, J.Y. Hwang, Q. Zhang, Y. Li, H. Wang, R.B. Kaner, 3D freeze-casting of cellular graphene films for ultrahigh-power-density supercapacitors, Adv. Mater. 28 (2016) 6719–6726.
[7] Z. Peng, R. Ye, J.A. Mann, D. Zakhidov, Y. Li, P.R. Smalley, J. Lin, J.M. Tour, Flexible boron-doped laser-induced graphene microsupercapacitors, ACS Nano 9 (6) (2015) 5868–5875.
[8] W. Gao, N. Singh, L. Song, Z. Liu, A.L.M. Reddy, L. Ci, R. Vajtai, Q. Zhang, B. Wei, P.M. Ajayan, Direct laser writing of micro-supercapacitors on hydrated graphite oxide films, Nat. Nanotechnol. 6 (8) (2011) 496–500.
[9] B. Wicklein, A. Kocjan, G. Salazar-Alvarez, F. Carosio, G. Camino, M. Antonietti, L. Bergström, Thermally insulating and fire-retardant lightweight anisotropic foams based on nanocellulose and graphene oxide, Nat. Nanotechnol. 10 (3) (2015) 277–283.
[10] J. Turkevich, The formation of colloidal gold, J. Phys. Chem. 57 (1953) 670–673.
[11] M. Maltez-da Costa, A. de la Escosura-Muñiz, A. Merkoçi, Electrochemical quantification of gold nanoparticles based on their catalytic properties toward hydrogen formation: application in magnetoimmunoassays, Electrochem. Commun. 12 (11) (2010) 1501–1504.
[12] L. Baptista-Pires, C.C. Mayorga-Martínez, M. Medina-Sánchez, H. Montón, A. Merkoçi, Water activated graphene oxide transfer using wax printed membranes for fast patterning of a touch sensitive device, ACS Nano 10 (1) (2016) 853–860.
[13] J. Garoz-Ruiz, A. Heras, S. Palmero, A. Colina, Development of a novel bidimensional spectroelectrochemistry cell using transfer single-walled carbon nanotubes films as optically transparent electrodes, Anal. Chem. 87 (2015) 6233–6239.
[14] E. Paramo, S. Palmero, A. Heras, A. Colina, Carbon nanostructured films modified by metal nanoparticles supported on filtering membranes for electroanalysis, Talanta 178 (2018) 736–742.
[15] R.S. Nicholson, Theory and application of cyclic voltammetry for measurement of electrode reaction kinetics, Anal. Chem. 37 (1965) 1351–1355.